A Meta-analysis to Revisit the Property-Aggregation Relationships of Carbon Nanomaterials: Experimental Observations Versus Predictions of the DLVO Theory

Bo Peng[1], Peng Liao[2], Yi Jiang[1]*

[1]Department of Civil and Environmental Engineering, The Hong Kong Polytechnic University, Kowloon, Hong Kong, China

[2] State Key Laboratory of Environmental Geochemistry, Institute of Geochemistry, Chinese Academy of Sciences, 99 Lingcheng West Road, Guiyang, 550081, China

March 2024

* To whom correspondence should be addressed:

Yi Jiang: Tel: +852-27666044; Fax: +852-23346389; Email: yi-cee.jiang@polyu.edu.hk

Abstract

Contradicting relationships between physicochemical properties of nanomaterials (e.g., size and zeta potential) and their aggregation behavior have been constantly reported in previous literature, and such contradictions deviate from the predictions of the classic Derjaguin, Landau, Verwey and Overbeek (DLVO) theory. To resolve such controversies, in this work, we employed a meta-analytic approach to synthesize the data from 46 individual studies reporting the critical coagulation concentration (CCC) of two carbon nanomaterials, namely, graphene oxide (GO) and carbon nanotube (CNT). The correlations between CCC and material physicochemical properties (i.e., size, zeta potential, and surface functionalities) were examined and compared with the theoretical predictions. Results showed that the CCC of electrostatically stabilized carbon nanomaterials increased with decreasing nanomaterial size when their hydrodynamic sizes were smaller than *ca.* 200 nm. This is qualitatively consistent with the prediction of the DLVO theory, but with a smaller threshold size than the predicted 2 μm. Above the threshold size, material zeta potential can be correlated to CCC for nanomaterials with moderate/low surface charge, in agreement with the DLVO theory. The correlation was not observed for highly charged nanomaterials because of their underestimated surface charge by zeta potential. Furthermore, a correlation between the C/O ratio and CCC was observed, where a lower C/O ratio resulted in a higher CCC. Overall, our findings rationalized the inconsistency between experimental observation and theoretical prediction, and provided essential insights into the aggregation behavior of nanomaterials in water, which could facilitate their rational design.

1. Introduction

Engineered nanomaterials are manufactured materials with at least one nanoscale dimension (*ca.* 1−100 nm). The high surface energy of nanomaterial often leads to uncontrolled aggregation, which affects not only their (designed) functionality (e.g., reduced reactivity[1, 2]) but also their toxicity, bioavailability, fate and transport in the environment.[3] As such, the aquatic aggregation behavior of various nanomaterials has been extensively studied over the past two decades.[4-8] Quantitative assessment of the aggregation behavior of nanomaterials was often performed by estimating their critical coagulation concentration (CCC) in quiescent electrolytes, where the Brownian motion induced particle collision. The CCC was obtained by monitoring the growth of nanomaterial size at the early stage of aggregation using time-resolved dynamic light scattering.[9] The CCC represents the minimum concentration of counterions required to fully destabilize the nanomaterial, where the aggregation is limited by Brownian diffusion.[10]

As the number of studies investigating the CCC of nanomaterials continues to grow, wide discrepancies in the reported CCC values are often observed, even for the same type of nanomaterial. For example, Yang et al. reported the CCC of graphene oxide (GO) in NaCl electrolyte as 36 mM,[11] while Kim et al. reported a value of 387.2 mM NaCl;[12] Xia et al. determined the CCC of multi-wall carbon nanotube (MWNT) to be 8.8 mM NaCl,[13] while Yi and Chen reported the CCC of MWNT as 210 mM NaCl.[14] Such variations are likely induced by the different physicochemical properties of the nanomaterials (varied size, surface charge, surface chemistry, etc.) in each study. Many nanomaterials, such as GO, can be more accurately recognized as a family of nanomaterials with different physicochemical properties.

Contradictory relationships between certain physicochemical properties of nanomaterials and their colloidal stability are often observed among studies. For instance, the CCC of GO was found to be negatively correlated to its material size.[15, 16] Similar effect of size on the CCC

has also been reported for other nanomaterials, such as CdSe,[17] hematite,[18] and silver nanomaterials.[19] The observed negative correlation between CCC and material size is consistent with an early prediction from the classic Derjaguin-Landau-Verwey-Overbeek (DLVO) theory.[20] However, the opposite trend has also been observed. Hematite[21] and TiO_2 nanomaterials[22] were reported to be more prone to aggregation as the size of nanomaterials became smaller, and the colloidal stability of gold nanomaterials was reported to be independent of their material size.[23]

In addition to material size, zeta potential, which is often used to infer the surface charge of nanomaterials,[24] has also been correlated to the CCC of nanomaterials based on the DLVO theory. The CCC is predicted to be proportional to the material surface potential, which is often approximated by the zeta potential, and a higher zeta potential results in a higher CCC.[25] This proportionality was demonstrated in our previous work, in which the CCCs of five reduced GOs were mathematically related to their zeta potential as predicted by the DLVO theory.[26] However, a few studies also observed significantly varied CCC of nanomaterials with similar zeta potential, deviating from the theoretical prediction. For example, Qi et al. reported that the CCC of GO in NaCl electrolyte was almost twice that of the L-ascorbic acid-reduced GO, whereas the zeta potential of these nanomaterials were similar (*ca.* -40 mV).[27] Likewise, although the zeta potential of three oxidized MWNTs were similar (*ca.* -60 mV), the CCC of these materials in NaCl electrolyte were 22.5, 57.9, and 108.1 mM, respectively.[28]

Studies have also been trying to correlate the material stability with surface chemistry, such as the surface oxidation degree for carbon nanomaterials. Both positive and negative correlations have been observed. For example, Qi et al. reported that the CCC of GO in NaCl electrolyte gradually decreased from 210 mM to 41 mM along with the increasing C/O ratio from 2.1 to 5.7,[27] whereas Gao et al. observed that GO with a higher C/O ratio (2.4) to be more stable than the one with a lower C/O ratio (1.2) in three common electrolytes (NaCl, $MgCl_2$,

and $CaCl_2$).[29] Azizighannad and Mitra found similar stability for GO with different oxidation degrees (C/O ratio = 1.0 and 2.1, respectively) in NaCl and $MgCl_2$ electrolytes.[30] Jiang et al. observed a positive correlation between the oxidation degree and the CCC of GO in $CaCl_2$ electrolyte,[26] while Xia et al. reported the opposite for MWNT.[13]

Altogether, the above-mentioned study-to-study variations on the property-aggregation relationships of nanomaterials suggest that research synthesis efforts are needed to identify whether there is a consistent relationship between a specific property of nanomaterials and their aggregation, and such work has been rarely performed. Furthermore, although the analytical expressions of the classic DLVO theory of colloid science are commonly used to interpret the aggregation behavior of nanomaterials,[31-33] it must be noted that these analytical expressions were obtained under certain assumptions, such as the Derjaguin approximation and/or the Debye−Hückel approximation.[20, 25, 34] Nanomaterial properties (such as small size and non-spherical shape) may not satisfy these assumptions, thus challenging the applicability of these analytical expressions.[1, 3] To resolve the inconsistency and examine the applicability, the data-driven research (e.g., meta-analysis) serves with great potential. Meta-analysis is an objective, quantitative, and powerful approach to synthesize findings across studies to determine patterns.[35] To date, according to the best of our knowledge, the use of a meta-analytic approach to examine the validity/applicability of the theoretical framework in interpreting the aggregation behavior of nanomaterials has yet to be performed.

In this study, we conducted a meta-analysis of 46 individual studies reporting the CCC of carbon nanomaterials and correlated their CCC in electrolytes and material intrinsic properties (i.e., size, zeta potential, and surface chemistry; the three most characterized properties). Specifically, we selected two types of carbon nanomaterials (i.e., graphene-based nanomaterials and carbon nanotubes) for the data-driven analysis because these materials with different physicochemical properties have been widely studied by multiple groups of

researchers over the past two decades. We aim to resolve the seemingly contradictory effects of physicochemical properties of nanomaterials on their aggregation behavior and examine the applicability of related theoretical predictions of CCC with regard to size and surface charge based on the DLVO theory. Overall, this meta-analytic approach will allow us to gain an improved understanding of the role of material physicochemical properties in determining the aggregation behavior of nanomaterials in water.

2. Methods

2.1 Data sources

We searched the Google Scholar database for publications that reported the critical coagulation concentration (CCC) of carbon nanomaterials (i.e., GO, multi- and single-wall carbon nanotubes (MWNT and SWNT)) by August 29th, 2022. Studies were identified with the search term "material critical coagulation concentration" (material refers to the carbon nanomaterials mentioned above). In the searching, only original research articles (i.e., excluding reviews) were retained and the language was restricted to English.

2.2 Study selection and eligibility criteria

After the studies were retrieved, full-text records were examined to assess their eligibility for analysis. Specifically, we applied two selection criteria: (1) the critical coagulation concentration (CCC) of nanomaterials was determined by time-resolved dynamic light scattering (TR-DLS) at pH 5-8 in quiescent electrolytes (excluding the effect of flow on CCC[36]); (2) nanomaterials were electrostatically stabilized (i.e., no surface coating of surfactant/polymer, etc.). Rationale for criterion 1 is that the CCC of nanomaterials could be determined by the TR-DLS method[6, 9] or the UV-vis method.[5, 37] Both methods measure the aggregation of nanomaterials at different electrolyte concentrations; the former obtains the CCC as the minimum electrolyte concentration at which nanomaterial aggregation is limited

by Brownian motion, while the latter determines the CCC at which the loss of absorbance reaches 0.5. The varied experimental approach could weaken the validity of comparison among studies. Rationale for criterion 2 is that the aggregation behavior of coated nanomaterials is largely determined by the properties of the surface coating rather than those of the 'bare' nanomaterial.[8, 38-43]

2.3 Data extraction

Nanomaterials properties and CCC in NaCl/$MgCl_2$/$CaCl_2$ electrolytes were extracted from the tables or from figures in selected publications using PlotDigitizer (https://plotdigitizer.com/). Typically, the physicochemical properties of nanomaterial reported in the literature include shape, size (hydrodynamic size measured by DLS and/or physical dimension examined by TEM/SEM/AFM), surface charge (zeta potential or electrophoretic mobility), and surface functionalities. Since the CCC was determined by TR-DLS, the hydrodynamic size determined by DLS was used for analysis in this study. The measured electrophoretic mobility is typically converted to zeta potential using the Smoluchowski equation.[7, 26] This estimated zeta potential is often used to infer the surface charge and predict the aggregation behavior of nanomaterials.[24] The zeta potential measured at a low ionic strength (1-10 mM NaCl) was used for analysis in this study. Surface functionalities, including the C/O ratio and fraction of different functional groups, were characterized by X-ray photoelectron spectroscopy (XPS). The fractions of functional groups (C-C/C-O/C=O/O-C=O) were obtained by deconvoluting the C1s spectra. The CCC of nanomaterial in NaCl/$MgCl_2$/$CaCl_2$ electrolytes, as well as the corresponding pH under which CCC was determined, was recorded for analysis. All the data are summarized in Table S1-S4 and Figure S1.

The surface charge of GO/rGO/MWNT obtained from potentiometric titration experiments were collected from individual studies and analyzed.[44-54] Titration experiment measures the

number of ionized groups on material. For GO and rGO, the surface charge density was calculated by assuming each ionized group carries one negative charge and a surface area of 1800 m^2/g.[31] For MWNT, the surface charge density was retrieved from Smith et al.[44]

2.4 Data analysis

Based on the C/O ratio from XPS measurement, graphene-based nanomaterials were further classified as GO and reduced GO (rGO). Materials with C/O ratio > 2.5 were classified as rGO, and those with C/O ratio < 2.5 were considered as GO.[55] For those studies that did not report XPS data, GO/rGO as indicated by the article was used for the classification.

The CCC values among different nanomaterials were compared using one-way ANOVA followed by the Tukey test. The correlation between the reported CCC values and material physicochemical properties was examined by the Spearman's rank correlation coefficient (ρ) for GO/rGO/MWNT (Table S5-S7), and SWNT was excluded for such analysis due to limited data. The coefficient varies between 1.0 (a perfect positive correlation) and -1.0 (a perfect negative correlation), and a value of 0 indicates no association between ranks. The results of the Spearman correlation are reported in the format of ρ [sample size], followed by the *p* value.

2.5 Analytical expressions from the DLVO theory

The DLVO theory assumes that the total interaction energy (V_T) of two particles is the sum of electric double layer repulsion (V_{EDL}) and van der Waals attraction (V_{vdW}). Since the methods used to characterize the hydrodynamic size and zeta potential of non-spherical nanomaterials treated them as spherical nanoparticles that have the same average translational diffusion coefficients,[15] we therefore used analytical expressions of interaction energy derived for spherical particles in the modeling. The use of sphere-sphere DLVO model for non-spherical nanomaterials has been demonstrated in previous individual studies and satisfactory results were reported.[12, 26, 43]

Assuming that the thickness of the electrical double layer is much smaller than the particle size, the Derjaguin approximation was applied to obtain the electrical potential energy between two spherical particles in *a:b* electrolyte:[25]

$$V_{EDL} = \frac{32(a+b)\pi X_0 n k_B T}{a k_3^2 \kappa^3}\left[\tanh^2\left(\frac{a\psi_0}{4}\right)\right]\exp(-k_3 L)\left[1-\frac{1}{2k_3 X_0}\left(1-\exp(-2k_3 X_0)\right)\right] \quad (1)$$

$$\psi_0 = \frac{e\Phi_0}{k_B T} \quad (2)$$

$$X_0 = \kappa r_0 \quad (3)$$

$$\kappa^2 = \frac{a(a+b)ne^2}{\varepsilon_0 \varepsilon_r k_B T} \quad (4)$$

where ψ_0 is dimensionless surface potential and Φ_0 is surface potential; X_0 is the dimensionless radius of particle and r_0 is particle radius; L is the surface-to-surface distance; κ is the reciprocal Debye length, ε_0 and ε_r are the permeability of vacuum and the relative permeability of water, respectively, T is the absolute temperature, e is the elementary charge, k_B is the Boltzmann constant; n is the number concentration of cations (nanomaterials surveyed in this study were all negatively charged) in bulk phase, and k_3 is a parameter related to valences of electrolyte: for NaCl, $k_3 = 1$; for $CaCl_2$ and $MgCl_2$, $k_3 \approx 1.078$.

The van der Waals potential can be estimated by:[25]

$$V_{vdW} = \frac{-A_{121} X_0}{12L} \quad (5)$$

where A_{121} is the Hamaker constant for the nanomaterial-water-nanomaterial system.

The total interaction energy V_T is the sum of V_{EDL} and V_{vdW}, and at CCC

$$V_T = 0 \text{ and } \frac{dV_T}{dL} = 0 \quad (6)$$

By solving equations (3), (5), and (6), CCC can be obtained:

$$n = \frac{\lambda \tanh^4\left(\frac{a\psi_0}{4}\right)}{a^5(a+b)k_3^6}\frac{(4\pi\varepsilon_0\varepsilon_r)^3(k_B T)^5 48^2}{e^6 {A_{121}}^2 \pi \exp(2)} \quad (7)$$

$$\lambda = \left[1-\frac{1}{2k_3 X_0}\left(1-exp(-2k_3 X_0)\right)\right]^2 \quad (8)$$

That is, CCC is proportional to the inverse of Hamaker constant and surface potential:

$$\frac{n}{\lambda} \propto \frac{1}{A_{121}^2} \tanh^4\left(\frac{a\psi_0}{4}\right) \quad (9)$$

For $X_0 \gg 1$, i.e., the assumption that the thickness of the electrical double layer (κ^{-1}) is much smaller than the particle radius (r_0), $\lambda \to 1$.

In the case when the thickness of an electrical double layer is not much smaller than the particle radius ($\kappa r_0 > 1$), the van der Waals potential between two spherical particles in Z:Z symmetric electrolyte can be estimated by:[20]

$$V_{vdW} = \frac{-A_{121}}{6}\left\{\frac{2r_0^2}{R^2-4r_0^2} + \frac{2r_0^2}{R^2} + \ln\left(\frac{R^2-4r_0^2}{R^2}\right)\right\} \quad (10)$$

where R is the center-to-center distance between two particles. The electrical potential energy can be approximated as:[20]

$$V_{EDL} = B\frac{r_0^2}{R}\ln\{1 + exp(-\kappa L)\}) \quad (11)$$

$$B = \varepsilon_0\varepsilon_r\left(\frac{k_BT}{Ze}\right)^2\left\{4\exp\left(\frac{\kappa L}{2}\right)\tanh^{-1}\left[\exp\left(\frac{-\kappa L}{2}\right)\tanh\left(\frac{Ze\psi_0}{4k_BT}\right)\right]\right\}^2 \quad (12)$$

An approximate solution of the inverse length at CCC could be obtained by solving Equation 6, 10, and 11:[20]

$$\kappa \cong \frac{8}{7}Q - \frac{80+128\ln\left(\frac{Lm}{r_0}\right)}{56r_0} \quad (13)$$

$$Q = \frac{6B}{A_{121}}\ln\left[1 + exp\left(-\frac{8}{7}\right)\right] \quad (14)$$

L_m is the closest surface-to-surface distance between two particles.

3. Results and Discussion

Our search identified 62 individual studies, and after the screening, 46 studies were included in our analysis.[6, 7, 11-16, 26, 27, 29, 30, 33, 41, 42, 44, 56-85] These studies reported the CCC of (electrostatically stabilized) nanomaterials in NaCl/$MgCl_2$/$CaCl_2$ electrolytes using TR-DLS. Figure 1 describes the details of the search and Table S1-S4 summarize the basic characteristics of nanomaterials studied in the included studies.

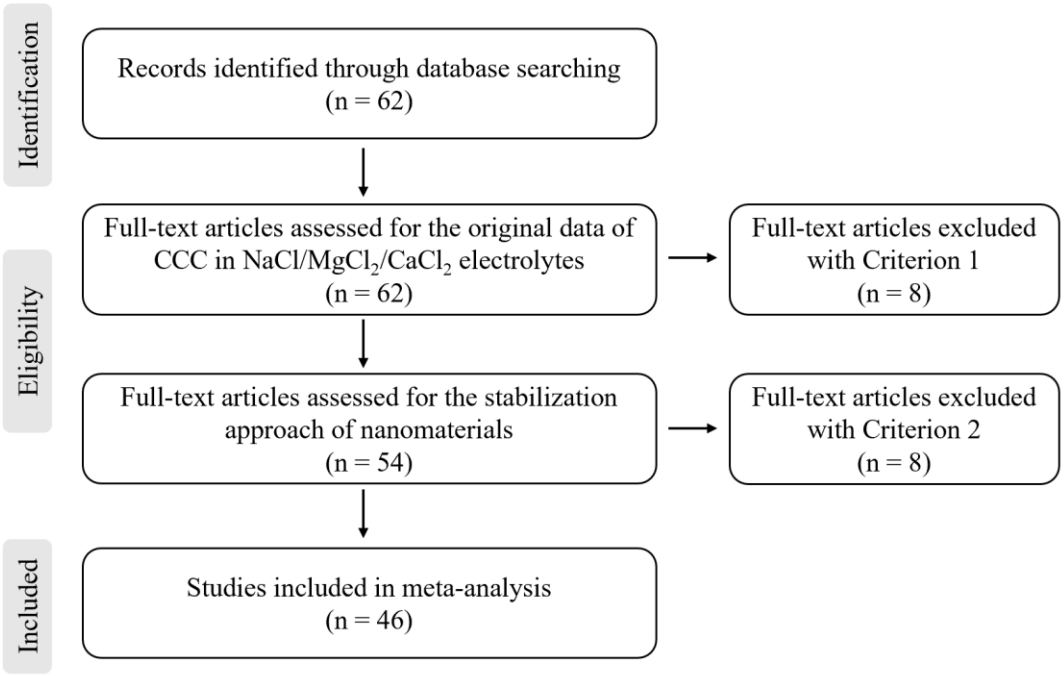

Figure 1. Study selection flow diagram. The two criteria used in the screening for eligibility are: Criterion 1, the critical coagulation concentration (CCC) of nanomaterials was determined in pH 5-8 via time-resolved dynamic light scattering; Criterion 2, nanomaterials were electrostatically stabilized (i.e., no surface coating of surfactant/polymer, etc.)

Figure 2 depicts the box plots of the CCC of each nanomaterial reported in these studies. The figures show that the CCC of the same type of nanomaterial could vary significantly from study to study. The NaCl CCC of GO ranged from 28 to 387.2 mM (Figure 2a), the $MgCl_2$ CCC of GO ranged from 1.2 to 19 mM (Figure 2b), and the $CaCl_2$ CCC ranged from 0.3 to 4.2 mM (Figure 2c). The much lower $MgCl_2$/$CaCl_2$ CCC than NaCl CCC could be attributed to that divalent counterions screen the electric double layer more efficiently than monovalent counterions and possible divalent cation bridging.[86] The experimental conditions for CCC determination were limited to a simple system consisting of nanomaterial and electrolyte, and the pH was in the range of 5-8. In the collected data, 18 out of 48 records reported the CCC of GO in pH 5.0-6.0, 12 out of 48 in pH 6.0-7.0, and 20 out of 48 in pH 7.0-8.0; 18 out of 21 records reported the rGO CCC in pH 6.0-7.0; all 42 records reported the CCC of MWNT in

pH 6.0-7.2; and all 4 records reported the CCC of SWNT in pH 6.0-7.0. Deprotonation of carboxyl and phenolic functional groups on the surface of these carbon nanomaterials mainly contribute to their surface charge.[26, 44] The pK_a of carboxyl group on aromatic rings is lower than 4.2 and the pK_a of phenolic group is around 10.[26] Therefore, within the pH range of 5-8, most of the carboxyl functional groups are deprotonated and the impact of pH on the CCC is minimum.[77] Furthermore, we have also analyzed the property-aggregation relationships of nanomaterials with a narrower pH range of 6.0-8.0 (data not shown) and the conclusions were consistent with those shown later in this work. As such, the varied CCC of the same type of nanomaterial was mainly attributed to the difference in the material intrinsic physicochemical properties. The Spearman's rank correlation coefficient between CCC and material physicochemical properties for GO/rGO/MWNT are presented in Table S5-S7, respectively. SWNT is excluded due to limited data. Below we discuss the correlation between the CCC and each of the physicochemical properties of the nanomaterials.

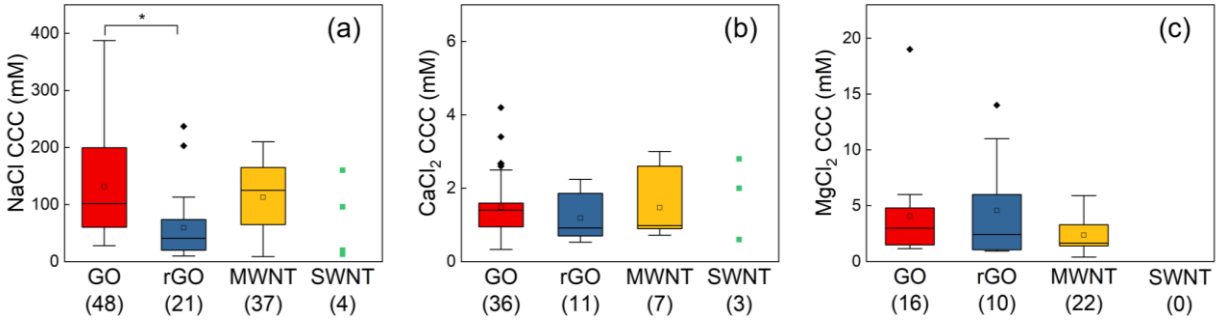

Figure 2. Box plots of critical coagulation concentrations (CCC) of carbon nanomaterials in (a) NaCl, (b) $CaCl_2$, and (c) $MgCl_2$ electrolytes under pH 5-8. Sample size of each box is shown in the corresponding bracket. Asterisks indicate a significant difference (one-way ANOVA test followed by the Tukey test for multiple comparisons, $p < 0.05$).

3.1 Correlation between CCC and nanomaterial size

The CCC of each nanomaterial versus its reported hydrodynamic size was plotted (Figure S2). Results of the Spearman correlation analysis indicated that there was a significant negative correlation between the NaCl CCC and hydrodynamic size of GO (ρ [40] = -0.54, $p < 0.001$) and MWNT (ρ [22] = -0.82, $p < 0.001$), but the negative correlation was not statistically significant for rGO (ρ [20] = -0.34, $p = 0.138$). Due to the limited data of SWNT, the Spearman correlation analysis was not performed. The insignificant correlation observed for rGO was because of the much varied zeta potential of rGO (from *ca.* -5 to -50 mV, Figure S1e), which may play a comparable or even more important role than the size does.[19] To minimize the impact from zeta potential, we analyzed rGO with similar zeta potential (Figure 3b) and observed a significant negative correlation between NaCl CCC and material size (ρ [9] = -0.84, $p = 0.009$). The negative correlation between the NaCl CCC and hydrodynamic size also existed for GO (ρ [21] = -0.48, $p = 0.033$) and MWNT (ρ [13] = -0.86, $p < 0.001$) when the condition of similar zeta potential was applied (Figure 3a and c). Due to the limited data of SWNT (only four data reported, Figure S2d), the relationship between NaCl CCC and material size cannot be established.

In divalent electrolytes, a negative correlation between the $MgCl_2$/$CaCl_2$ CCC and the hydrodynamic size can also be observed for GO, rGO, and MWNT by analyzing the nanomaterials with similar zeta potential (Figure 3d-i). The Spearman correlation analysis indicated a significant negative correlation between the CCC and hydrodynamic size for GO in $MgCl_2$ (ρ [9] = -0.69, $p = 0.038$) and $CaCl_2$ (ρ [26] = -0.64, $p = 0.002$), rGO in $MgCl_2$ (ρ [5] = -0.97, $p = 0.005$), and MWNT in $MgCl_2$ (ρ [9] = -0.80, $p = 0.009$). rGO and MWNT in $CaCl_2$ were not analyzed due to limited data. If the condition of similar zeta potential was not applied, the correlation between $MgCl_2$/$CaCl_2$ CCC and hydrodynamic size became weaker (Table S5-7), since both surface charge and material size were influencing the nanomaterial stability.

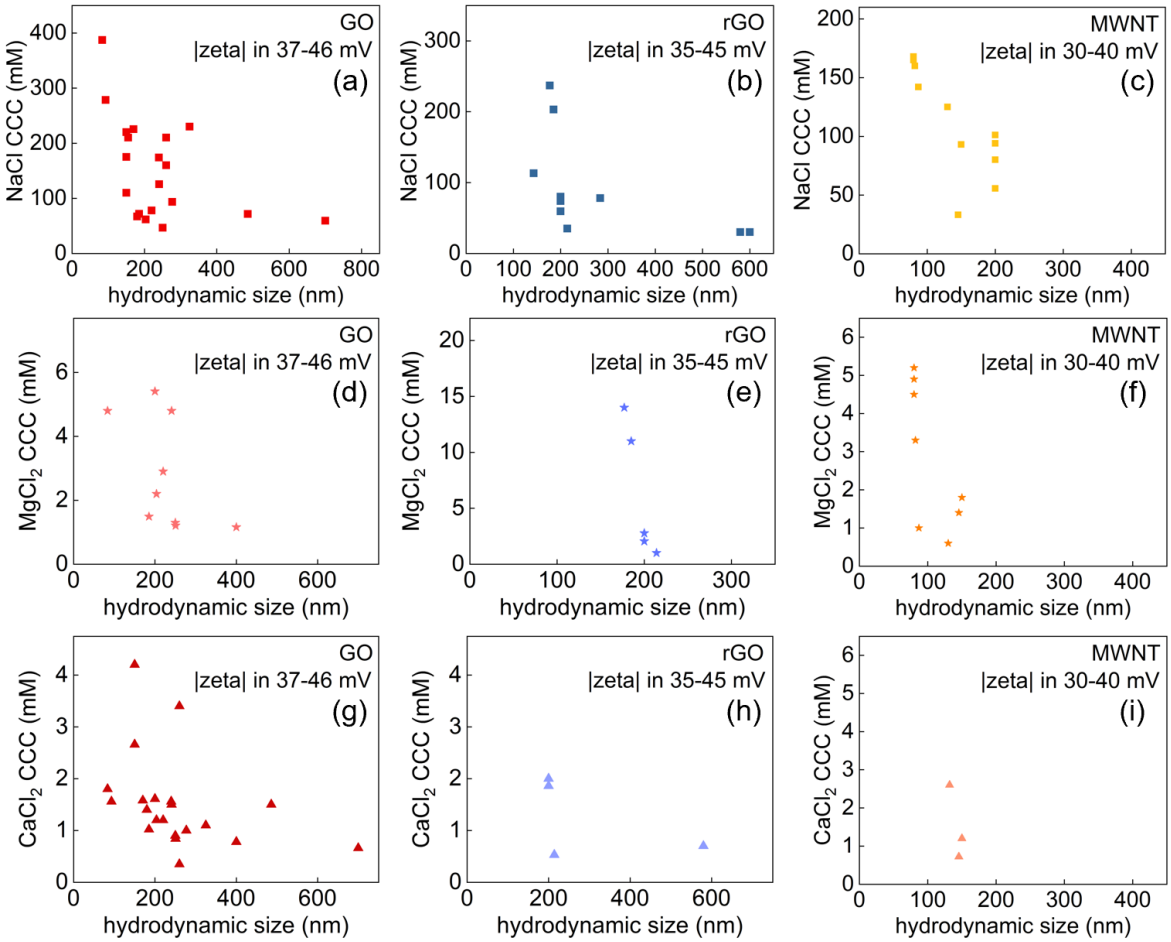

Figure 3. The critical coagulation concentration (CCC) of GO, rGO, and MWNT in (a-c) NaCl, (d-f) $MgCl_2$, and (g-i) $CaCl_2$ electrolytes are plotted as a function of their hydrodynamic size. The data was selected for nanomaterials with a narrow range of zeta potential (GO: -37-46 mV, rGO: -35-45 mV; MWNT: -30-40 mV).

The relationship between CCC and nanomaterial size has also been investigated in previous individual studies. Sun et al. reported an increased NaCl CCC with decreasing lateral size of GO (from 1000 to 200 nm, corresponding to hydrodynamic size from 240 to 93 nm), and the zeta potentials of these nanomaterials with different sizes were similar (*ca.* -42 mV).[15] Our conclusion was consistent with theirs. For MWNT, contradicting effects of material size were reported. While Ntim et al. observed the shorter MWNT (correspondingly smaller hydrodynamic size) possessed a higher CCC than the longer one,[74] Wu et al. reported the longer

315 MWNT was more stable in electrolyte.[60] The contradiction was likely due to the varied zeta
316 potentials of MWNT along with size (*ca.* -30 mV for the short one and -38 mV for the long
317 one) in Wu et al.'s work, whereas the zeta potentials of nanomaterials with different sizes were
318 similar (*ca.* -27 mV) in Ntim et al.'s work. The negative correlation between NaCl CCC and
319 particle size has also been observed for non-carbon nanomaterials.[17-19] For example, Afshinnia
320 et al. examined the CCC of silver nanomaterials (Ag NMs) from 11 research articles and
321 concluded that the CCC of Ag NMs increased with decreasing particle size at fixed zeta
322 potential.[19]

323 Nanomaterial aggregation is often interpreted based on the DLVO theory. Theoretical work
324 by Hsu and Liu predicted the CCC to be inversely related to particle size when the particle is
325 smaller than 2 μm.[20] However, we observed that the effect of size on CCC became prominent
326 below *ca.* 200 nm. A few reasons contribute to the observed discrepancy on the threshold size.
327 Firstly, it should be noted that the hydrodynamic size determined by DLS was used in our
328 analysis. For non-spherical nanomaterials, this approach reports the size of equivalent spherical
329 nanoparticles with the same translational diffusion coefficient as the non-spherical
330 nanomaterials, therefore the hydrodynamic size is not the actual physical size of non-spherical
331 nanomaterials, which is different from the physical size used in the theoretical work of Hsu
332 and Liu. For example, GO with hydrodynamic sizes of 240, 170, 128, 93 nm corresponded to
333 the average lateral sizes of 1000, 500, 350, 200 nm determined by FESEM, respectively.[15] Also,
334 the hydrodynamic size of long MWNT (10-20 μm) increased from *ca.* 200 nm to 500 nm as
335 the tube diameter increased from *ca.* 10 nm to 50 nm.[74] Nevertheless, the change in the
336 hydrodynamic size generally coincides with the change in the actual physical size of the
337 nanomaterials. Secondly, the observed discrepancy from the theoretical prediction may be due
338 to the lower dimensionality of carbon nanomaterials, which differs from the three-dimensional
339 (3D) nanoparticles used in the theoretical work of Hsu and Liu.[20] For example, the 2D nature

of GO and rGO has been shown to significantly affect the van der Waals forces, and the colloidal stability of 2D nanomaterials is less sensitive to the changes in the surface charge density compared to the 3D nanomaterials.[31] Although the 1D/2D nature of carbon nanomaterials might contribute to the deviation from the theoretical prediction, the threshold (hydrodynamic) size of spherical 3D silver nanomaterials was observed to be *ca.* 50 nm.[19] The deviation of experimental observations from the prediction of the DLVO theory thus requires more (theoretical) efforts to uncover the cause(s).

3.2 Correlation between CCC and surface charge (zeta potential)

3.2.1 Experimental observation vs. prediction based on the DLVO theory

Based on the DLVO theory, the CCC of nanomaterials could be mathematically correlated with material surface potential,[10, 25, 34, 87] and zeta potential is typically used as an approximation of surface potential in practice.[26, 31, 88] However, it should be noted that assumptions were made to simplify the derivation and to obtain the analytical expressions (e.g., Equation 9). While these assumptions are valid for (large) colloidal nanoparticles, they may fail for nanomaterials.[1] For example, Equation 9 was obtained by applying the Derjaguin approximation, which only holds when the thickness of the electrical double layer is much smaller than the particle size (i.e., $\kappa r_0 >> 1$).[10] Under such assumption, the analytical expression of CCC is independent of nanomaterial size.[20] This seemingly contradicts our observed effect of size on CCC as discussed above. Nevertheless, the theoretical work by Hsu and Liu suggests that there is a threshold size, beyond which the effect of size is minimum on the CCC.[20] We observed a threshold (hydrodynamic) size of *ca.* 200 nm (Figure 3).

The NaCl CCC of rGO with hydrodynamic size larger than 200 nm (solid squares in Figure 4b) was proportional to $\tanh^4\left(\frac{a\psi_0}{4}\right)$ when assuming the same Hamaker constant (A_{121}) values for the rGO (dash line in Figure 4b). However, the inclusion of rGO with a size smaller than

200 nm (open squares in Figure 4b) significantly weakened the correlation (dash-dot line in Figure 4b). A similar trend was observed for MWNT as well, but with a smaller threshold size of *ca.* 150 nm (Figure 4c). However, GO was an exception. A poor correlation between the CCC and zeta potential was observed even for GO with a hydrodynamic size larger than 200 nm (Figure 4a). The deviation from the theoretical prediction was likely due to the underestimated zeta potential of GO, which will be discussed in detail in the next section. The observed correlation between material zeta potential and CCC of rGO and MWNT is consistent with our earlier work, in which we observed a good correlation between the NaCl CCC and zeta potential of five rGO with similar hydrodynamic sizes of *ca.* 200 nm.[26]

It must be noted that the classic DLVO theory only considers electrostatic repulsion and van der Waals attraction, and Equation 9 was derived under the interaction of two spherical particles. Therefore, the deviation from the theoretical prediction may be also related to the factors not considered in the classic DLVO theory, such as other material properties (e.g., shape, orientation,[89, 90] and lattice characteristics[78]) and non-DLVO forces (such as hydrophobic interaction and hydrogen bonding). However, the observed consistence between experiment and theoretical prediction for rGO and MWNT with size larger than the threshold size (Figure 4b-c) suggests that the classic DLVO theory is adequate to, at least, roughly predict their aggregation behavior, and a more accurate prediction would require more sophisticated characterization of the material and the inclusion of non-DLVO forces.

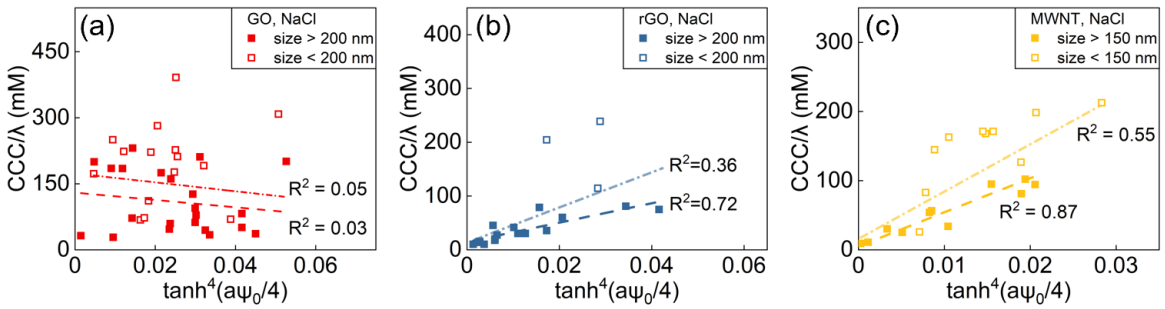

Figure 4. Correlation between the NaCl CCC and zeta potential of (a) GO, (b) rGO, and (c) MWNT based on the DLVO theory. Dash lines are the regression lines for solid squares only and dash-dot lines are the regression lines for all data (solid and open squares).

The relationship between CCC and material zeta potential in divalent electrolytes was not mathematically consistent with the theoretical prediction, except for MWNT in $MgCl_2$ electrolyte (Figure S3). Nevertheless, a qualitative trend was observed for both rGO and MWNT in $MgCl_2$ electrolyte, that is, a higher zeta potential leads to a higher $MgCl_2$ CCC of the nanomaterials (Figure S3a-b). However, distinct effects of Ca^{2+} on the CCC of rGO and MWNT were observed (Figure S3c-d). The $CaCl_2$ CCC of rGO tended to increase with zeta potential, whereas the $CaCl_2$ CCC of MWNT tended to be independent with zeta potential. This discrepancy was likely because the oxygen-containing functional groups on carbon nanomaterials surface could serve as effective binding sites for cation bridging,[13, 15] and such interaction was not considered in the classic DLVO theory. It should be noted that the mechanism of the divalent cation bridging has yet to be explicitly revealed. Previous studies suggest that the density[91] and position[92] of carboxyl groups play a role, as well as the species and concentration of divalent cations.[8] More efforts are required to fully understand the bridging mechanism(s).

3.2.2 Underestimated surface charge of GO by zeta potential

Although zeta potential is typically used to infer surface potential in practice, it must be noted that zeta potential is a modeled value based on measurement of electrophoretic mobility

using the electrophoretic light scattering method.[24] For example, the reported zeta potential of nanomaterials studied in this work was modeled using the Smoluchowski equation. Limitations lied within the electrophoretic light scattering method and the modeling approach may lead to the reported zeta potential not accurately indicating the surface charge of GO.

The negative surface charges of carbon nanomaterials are generally considered to originate from the oxygen-containing functional groups (e.g., carboxyl and hydroxyl groups).[26, 44, 46] The higher the oxidation degree, the more negative the surface charge of nanomaterials. However, by comparing the oxidation degree (indicated by the C/O ratio measured by XPS) of nanomaterials (only GO/rGO/MWNT have sufficient data for a quantitative comparison) and their zeta potential, we observed that the absolute zeta potential of graphene-based nanomaterial (GO and rGO) first increased with decreasing C/O ratio (from *ca.* 6 to 3), then reached a plateau and did not change with further decrease of the C/O ratio (from *ca.* 3-1) (Figure 5a). This plateau was not observed for MWNT, whose C/O ratio was all higher than 8 (Figure 5b). The Spearman correlation results also indicated that there was a significant correlation between the C/O ratio and zeta potential for rGO (ρ [15] = 0.55, p = 0.033) and MWNT (ρ [18] = 0.68, p = 0.002), but not for GO (ρ [31] = 0.25, p = 0.195). Therefore, we hypothesized that the measured zeta potential of highly charged nanomaterials may have underestimated their actual surface charge (e.g., C/O ratio < 3 for GO/rGO). To support this hypothesis, we synthesized the data of surface charges of GO/rGO/MWNT obtained from potentiometric titration experiments in published individual studies[31, 45-54] and plotted them against the C/O ratios in Figure 5c-d. Results from the titration method suggested the surface charge of both graphene-based nanomaterials (GO and rGO) (Spearman's ρ [15] = -0.78, p < 0.001) and MWNT (Spearman's ρ [11] = -0.95, p < 0.001) increased monotonically with the decreasing C/O ratio. The observed relationship is consistent with previous individual studies.[44, 93]

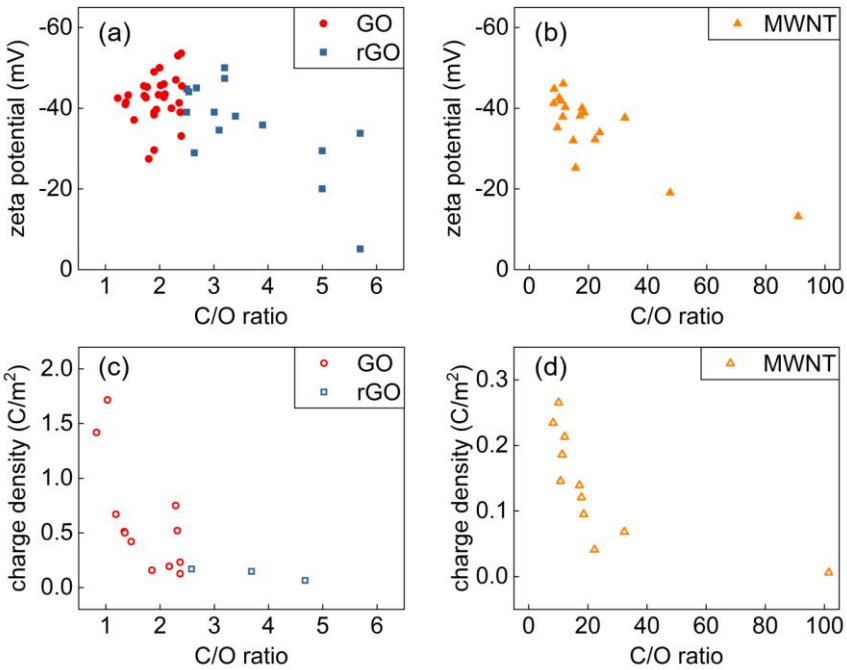

Figure 5. (a-b) Zeta potential are plotted against C/O ratio determined by XPS: (a) GO and rGO and (b) MWNT; (c-d) surface charge density against C/O ratio: (c) GO and rGO and (d) MWNT.

The disagreement between zeta potential from the electrophoretic light scattering measurement and charge density from the titration measurement may be due to two reasons. On one hand, the measurement of zeta potential depends on the light scattering of nanomaterials, but small nanomaterials (< 2-3 nm) do not scatter light. It should be noted that the oxidation of graphene and CNT not only generates oxygen-containing functional groups on material surface, but also produces molecular debris (i.e., oxidation debris, OD) that strongly adhere to the oxidized material.[94-96] These OD are too small to scatter light, therefore the charges from OD might not be detected in a zeta potential measurement, yet the charges of OD could be measured by titration.[46] On the other hand, it might not be appropriate to use the Smoluchowski equation to estimate the zeta potential of nanomaterial with high surface charge. Although this equation has been widely used in the literature to calculate the zeta potential

from electrophoretic mobility for various nanomaterials,[17, 19, 32, 33, 41] it must be noted that there are limitations to its use. The equation can be applied to a particle of arbitrary shape provided that the radii of surface curvature were everywhere much larger than the double layer thickness (κ^{-1}).[87] Only in the case of $\kappa r_0 > 20$ and moderate/low surface charge (e.g., absolute zeta potential ≤ 50 mV) can one safely apply the Smoluchowski equation.[97] If the surface charge is rather high (absolute zeta potential > 50 mV), the zeta potential is underestimated using the Smoluchowski equation and one needs to use more elaborate models (e.g., the numerical solutions by O'Brien and White).[97] Therefore, the inappropriate use of the Smoluchowski equation for GO with high surface charge (i.e., C/O ratio < 3) may contribute to the disagreement of measured zeta potential and charge density results.

3.3 Correlation between CCC and surface functionalities

Previous individual studies have observed a linear correlation between the carboxyl group and aqueous stability (i.e., CCC) of these carbon nanomaterials.[26, 28, 44, 59, 62] For example, we previously observed that the carboxyl groups (from *ca*. 3-5%) were highly correlated to the CCC of GO with different degrees of reduction (C/O ratio from *ca*. 2-5).[26] This positive correlation between the carboxyl groups and GO stability was supported by molecular dynamics simulation by Tang et al.[62] Similarly, the correlation between carboxyl groups and the CCC of MWNT has also been reported, in which the carboxyl content varied from *ca.* 1.5-5.5% for MWNT with different oxidation degrees (C/O ratio from 8-32).[44] However, in this meta-analysis we did not observe a significant correlation between the CCC and the carboxyl functional groups for none of these carbon nanomaterials (Figure S4 and Table S5-7). We postulated that this discrepancy might be caused by the varied approaches in deconvoluting the XPS spectra across studies. For example, the deconvolution of high-resolution C1s spectra were performed to account for either three oxygen-containing functional groups (i.e., C-C, C-O, and C=O),[75, 85] or four functional groups (i.e., C-C, C-O, C=O, and COOH),[15, 84] or five

functional groups (i.e., C-C, C-OH, C-O-C, C=O, and COOH).[26, 79] Varied rules applied in each study may cause errors in recognizing the surface functionalities of nanomaterials, especially when the carboxyl content only varied in a small range, e.g., from *ca.* 2-5% of GO[26] and *ca.* 1.5-5.5% of MWNT.[44] Therefore, unless a unified deconvolution method is applied to analyze the XPS spectra in each study, solid conclusion(s) on the correlation between the fractions of surface functionalities of nanomaterials and their aqueous stability might not be obtained.

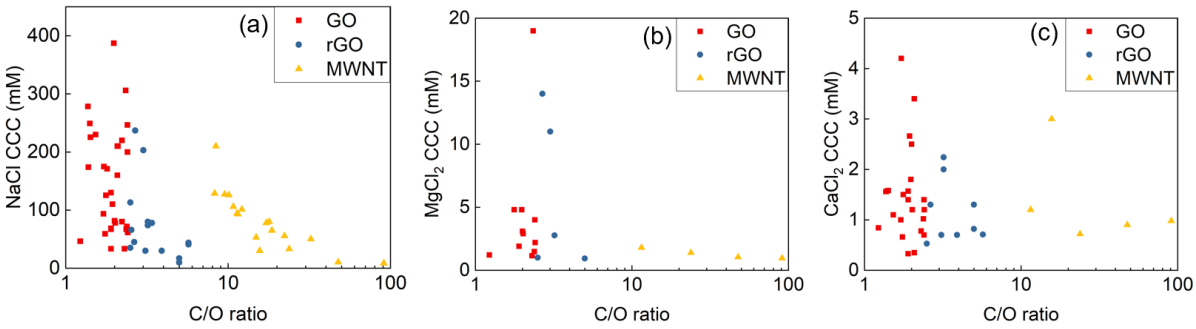

Figure 6. The critical coagulation concentration (CCC) of GO/rGO/MWNT in (a) NaCl, (b) $MgCl_2$, and (c) $CaCl_2$ electrolytes are plotted against the C/O ratio of these nanomaterials.

Nevertheless, the C/O ratio obtained by XPS did not require sophisticated deconvolution as the surface functionalities did, and we observed a general trend that the smaller the C/O ratio, the higher the NaCl CCC values for GO, rGO, and MWNT (Figure 6a). This is consistent with the observations in individual studies.[13, 14, 26, 44] Nonetheless, the correlation became weaker with decreasing C/O ratio (i.e., a higher oxidation degree) as indicated by the Spearman correlation (MWNT: ρ [18] = -0.92, $p < 0.001$; rGO: ρ [15] = -0.463, $p = 0.082$; GO: ρ [31] = -0.10, $p = 0.586$). In divalent electrolytes, the correlation between CCC and C/O ratio was much weaker (Figure 6b-c and Table S5-7). Compared with monovalent counterion, divalent cation has a stronger association with the nanomaterial and can possibly form bridges with the

carboxyl groups.[62] On one hand, the carboxyl group stabilizes the nanomaterial by providing negative charges. On the other hand, bridging interaction promotes nanomaterial aggregation. Therefore, in divalent electrolytes, the correlation between CCC and the C/O ratios became blurred.

4. Implications

Data-driven research has received wide attention in the scientific community and has great potential in improving the design of materials.[98-100] This study serves as a proof-of-concept for applying a meta-analytic approach to synthesize pre-existing data to determine patterns and make predictions, thereby obtaining a better understanding of the property-aggregation relationships of nanomaterials, which will be required for the development of accurate predictive models to estimate nanomaterial aggregation. This meta-analysis focused on the carbon nanomaterials, and future analysis can include more types of nanomaterials (e.g., metal nanoparticles and nanoplastics) to evaluate the generalizability of the findings in this analysis. Besides, with more data being integrated for the analysis, other factors affecting the aggregation behavior of nanomaterials, such as other properties of nanomaterials (e.g., shape, orientation,[89] surface coating, lattice characteristics,[78] the presence of impurity from synthesis), mixing flow,[36] non-DLVO forces, could be included in the analysis to produce a more accurate prediction of the aggregation behavior of nanomaterials. Other than the aggregation behavior of nanomaterials, their electronic structure and chemical activity are also property-dependent, and leveraging a meta-analytic approach to discover and define such relationships is well-suited.[100] Also, with more data being generated, future studies could utilize more advanced meta-analytic techniques, such as machine learning[98, 99] to better understand the interplay of multiple properties on the aggregation of nanomaterials and to provide potential practical aid in the design of nanomaterials.

5. Conclusion

In this work, we employed a meta-analytic approach to synthesize the available data from 46 individual studies and examined the correlation between material physicochemical properties (i.e., size, surface charge, surface functionalities) and their CCC in three electrolytes (i.e., NaCl/$MgCl_2$/$CaCl_2$). We conclude that the CCC of these carbon nanomaterials increases with decreasing nanomaterial size, and the effect of size becomes prominent when the hydrodynamic size is smaller than *ca.* 200 nm. This observation is qualitatively consistent with the early prediction of the DLVO theory, but with a smaller threshold size. Above the threshold size, material zeta potential can be correlated to CCC in NaCl electrolyte ($CCC/\lambda \propto \tanh^4\left(\frac{a\psi_0}{4}\right)$). The correlation is not observed in the divalent electrolytes, because divalent cation bridging, which may have occurred, was not considered in the framework of the DLVO theory. Although the zeta potential (obtained via the Smoluchowski equation) is commonly used to represent material surface charge, it only remains valid for nanomaterial with moderate/low surface charge (e.g., GO with C/O ratio > *ca.* 3 and MWNT with C/O ratio > 8). For GO with C/O ratio smaller than *ca.* 3, the measured zeta potential may underestimate the actual surface charge, thereby leading to the deviation of experimental observations from the prediction of the DLVO theory. With more oxygen-containing functional groups (i.e., lower C/O ratio), these carbon nanomaterials are more stable in water. However, the correlation with a specific functional group could not be established unless they are identified with a unified characterization approach across studies. Overall, our findings rationalize the inconsistency among previous observations of certain physicochemical properties on nanomaterial aggregation and provide essential insights into their aggregation behavior in water, thereby assisting their rational design for various applications.

Supporting Information

Nanomaterial physicochemical properties and critical coagulation concentration (CCC) extracted from the literatures; Spearman's correlation coefficient between CCC and material properties.

Acknowledgement

This work was supported by Hong Kong Research Grants Council's Early Career Award (25209819) and Science, Technology and Innovation Commission of Shenzhen Municipality (SGDX20210823103401009). The authors thank Dr. Danmeng Shuai (George Washington University) and Dr. Yandi Hu (Peking University) for their valuable comments during the writing phase of this paper.

Reference

1. Hotze, E. M.; Phenrat, T.; Lowry, G. V., Nanoparticle Aggregation: Challenges to Understanding Transport and Reactivity in the Environment. *J. Environ. Qual.* **2010,** *39* (6), 1909-1924.
2. Vikesland, P. J.; Heathcock, A. M.; Rebodos, R. L.; Makus, K. E., Particle Size and Aggregation Effects on Magnetite Reactivity toward Carbon Tetrachloride. *Environ. Sci. Technol.* **2007,** *41* (15), 5277-5283.
3. Baalousha, M., Effect of nanomaterial and media physicochemical properties on nanomaterial aggregation kinetics. *NanoImpact* **2017,** *6*, 55-68.
4. Chen, K. L.; Mylon, S. E.; Elimelech, M., Aggregation Kinetics of Alginate-Coated Hematite Nanoparticles in Monovalent and Divalent Electrolytes. *Environ. Sci. Technol.* **2006,** *40* (5), 1516-1523.
5. Sano, M.; Okamura, J.; Shinkai, S., Colloidal Nature of Single-Walled Carbon Nanotubes in Electrolyte Solution: The Schulze−Hardy Rule. *Langmuir* **2001,** *17* (22), 7172-7173.
6. Saleh, N. B.; Pfefferle, L. D.; Elimelech, M., Aggregation Kinetics of Multiwalled Carbon Nanotubes in Aquatic Systems: Measurements and Environmental Implications. *Environ. Sci. Technol.* **2008,** *42* (21), 7963-7969.
7. Wu, L.; Liu, L.; Gao, B.; Muñoz-Carpena, R.; Zhang, M.; Chen, H.; Zhou, Z.; Wang, H., Aggregation Kinetics of Graphene Oxides in Aqueous Solutions: Experiments, Mechanisms, and Modeling. *Langmuir* **2013,** *29* (49), 15174-15181.
8. Peng, B.; Liu, Z.; Jiang, Y., Aggregation of DNA-grafted nanoparticles in water: the critical role of sequence-dependent conformation of DNA coating. *J. Phys. Chem. B* **2022,** *126* (4), 847-857.
9. Chen, K. L.; Elimelech, M., Aggregation and Deposition Kinetics of Fullerene (C60) Nanoparticles. *Langmuir* **2006,** *22* (26), 10994-11001.
10. Elimelech, M.; Gregory, J.; Jia, X., *Particle Deposition and Aggregation: Measurement, Modelling and Simulation*. Butterworth-Heinemann: 1995.
11. Yang, K.; Chen, B.; Zhu, X.; Xing, B., Aggregation, Adsorption, and Morphological Transformation of Graphene Oxide in Aqueous Solutions Containing Different Metal Cations. *Environ. Sci. Technol.* **2016,** *50* (20), 11066-11075.
12. Kim, C.; Lee, J.; Wang, W.; Fortner, J., Organic Functionalized Graphene Oxide Behavior in Water. *Nanomaterials* **2020,** *10* (6), 1228.
13. Xia, T.; Guo, X.; Lin, Y.; Xin, B.; Li, S.; Yan, N.; Zhu, L., Aggregation of oxidized multi-walled carbon nanotubes: Interplay of nanomaterial surface O-functional groups and solution chemistry factors. *Environ. Pollut.* **2019,** *251*, 921-929.
14. Yi, P.; Chen, K. L., Influence of Surface Oxidation on the Aggregation and Deposition Kinetics of Multiwalled Carbon Nanotubes in Monovalent and Divalent Electrolytes. *Langmuir* **2011,** *27* (7), 3588-3599.
15. Sun, B.; Zhang, Y.; Liu, Q.; Yan, C.; Xiao, B.; Yang, J.; Liu, M.; Zhu, L., Lateral size dependent colloidal stability of graphene oxide in water: impacts of protein properties and water chemistry. *Environ. Sci.: Nano* **2020,** *7* (2), 634-644.
16. Szabo, T.; Maroni, P.; Szilagyi, I., Size-dependent aggregation of graphene oxide. *Carbon* **2020,** *160*, 145-155.
17. Mulvihill, M. J.; Habas, S. E.; Jen-La Plante, I.; Wan, J.; Mokari, T., Influence of Size, Shape, and Surface Coating on the Stability of Aqueous Suspensions of CdSe Nanoparticles. *Chem. Mater.* **2010,** *22* (18), 5251-5257.
18. Sheng, A.; Liu, F.; Shi, L.; Liu, J., Aggregation Kinetics of Hematite Particles in the Presence of Outer Membrane Cytochrome OmcA of Shewanella oneidenesis MR-1. *Environ. Sci. Technol.* **2016,** *50* (20), 11016-11024.

19. Afshinnia, K.; Sikder, M.; Cai, B.; Baalousha, M., Effect of nanomaterial and media physicochemical properties on Ag NM aggregation kinetics. *J. Colloid Interface Sci.* **2017,** *487*, 192-200.
20. Hsu, J.-P.; Liu, B.-T., Effect of Particle Size on Critical Coagulation Concentration. *J. Colloid Interface Sci.* **1998,** *198* (1), 186-189.
21. He, Y. T.; Wan, J.; Tokunaga, T., Kinetic stability of hematite nanoparticles: the effect of particle sizes. *J. Nanopart. Res.* **2008,** *10* (2), 321-332.
22. Zhou, D.; Ji, Z.; Jiang, X.; Dunphy, D. R.; Brinker, J.; Keller, A. A., Influence of Material Properties on TiO2 Nanoparticle Agglomeration. *PLOS ONE* **2013,** *8* (11), e81239.
23. Liu, J.; Legros, S.; Ma, G.; Veinot, J. G. C.; von der Kammer, F.; Hofmann, T., Influence of surface functionalization and particle size on the aggregation kinetics of engineered nanoparticles. *Chemosphere* **2012,** *87* (8), 918-924.
24. Lowry, G. V.; Hill, R. J.; Harper, S.; Rawle, A. F.; Hendren, C. O.; Klaessig, F.; Nobbmann, U.; Sayre, P.; Rumble, J., Guidance to improve the scientific value of zeta-potential measurements in nanoEHS. *Environ. Sci.: Nano* **2016,** *3* (5), 953-965.
25. Hsu, J.-P.; Kuo, Y.-C., The critical coagulation concentration of counterions: Spherical particles in asymmetric electrolyte solutions. *J. Colloid Interface Sci.* **1997,** *185* (2), 530-537.
26. Jiang, Y.; Raliya, R.; Fortner, J. D.; Biswas, P., Graphene Oxides in Water: Correlating Morphology and Surface Chemistry with Aggregation Behavior. *Environ. Sci. Technol.* **2016,** *50* (13), 6964-6973.
27. Qi, Y.; Xia, T.; Li, Y.; Duan, L.; Chen, W., Colloidal stability of reduced graphene oxide materials prepared using different reducing agents. *Environ. Sci.: Nano* **2016,** *3* (5), 1062-1071.
28. Bai, Y.; Wu, F.; Lin, D.; Xing, B., Aqueous stabilization of carbon nanotubes: effects of surface oxidization and solution chemistry. *Environ. Sci. Pollut. Res.* **2014,** *21* (6), 4358-4365.
29. Gao, Y.; Ren, X.; Song, G.; Chen, D.; Zhang, X.; Chen, C., Colloidal properties and stability of UV-transformed graphene oxide in aqueous solutions: The role of disorder degree. *J. Hazard. Mater.* **2020,** *382*, 121097.
30. Azizighannad, S.; Mitra, S., Stepwise Reduction of Graphene Oxide (GO) and Its Effects on Chemical and Colloidal Properties. *Sci. Rep.* **2018,** *8* (1), 10083.
31. Gudarzi, M. M., Colloidal Stability of Graphene Oxide: Aggregation in Two Dimensions. *Langmuir* **2016,** *32* (20), 5058-5068.
32. Omija, K.; Hakim, A.; Masuda, K.; Yamaguchi, A.; Kobayashi, M., Effect of counter ion valence and pH on the aggregation and charging of oxidized carbon nanohorn (CNHox) in aqueous solution. *Colloids Surf. A Physicochem. Eng. Asp.* **2021,** *619*, 126552.
33. Chowdhury, I.; Duch, M. C.; Mansukhani, N. D.; Hersam, M. C.; Bouchard, D., Colloidal Properties and Stability of Graphene Oxide Nanomaterials in the Aquatic Environment. *Environ. Sci. Technol.* **2013,** *47* (12), 6288-6296.
34. Trefalt, G.; Szilagyi, I.; Téllez, G.; Borkovec, M., Colloidal Stability in Asymmetric Electrolytes: Modifications of the Schulze–Hardy Rule. *Langmuir* **2017,** *33* (7), 1695-1704.
35. Gurevitch, J.; Koricheva, J.; Nakagawa, S.; Stewart, G., Meta-analysis and the science of research synthesis. *Nature* **2018,** *555* (7695), 175-182.
36. Gao, J.; Sugimoto, T.; Kobayashi, M., Effects of ionic valence on aggregation kinetics of colloidal particles with and without a mixing flow. *J. Colloid Interface Sci.* **2023,** *638*, 733-742.
37. Lin, D.; Liu, N.; Yang, K.; Zhu, L.; Xu, Y.; Xing, B., The effect of ionic strength and pH on the stability of tannic acid-facilitated carbon nanotube suspensions. *Carbon* **2009,** *47* (12), 2875-2882.

38. Peng, B.; Liao, P.; Jiang, Y., Preferential interactions of surface-bound engineered single stranded DNA with highly aromatic natural organic matter: Mechanistic insights and implications for optimizing practical aquatic applications. *Water Res.* **2022,** *223*, 119015.
39. Louie, S. M.; Tilton, R. D.; Lowry, G. V., Effects of molecular weight distribution and chemical properties of natural organic matter on gold nanoparticle aggregation. *Environ. Sci. Technol.* **2013,** *47* (9), 4245-4254.
40. Chang, X.; Henderson, W. M.; Bouchard, D. C., Multiwalled Carbon Nanotube Dispersion Methods Affect Their Aggregation, Deposition, and Biomarker Response. *Environ. Sci. Technol.* **2015,** *49* (11), 6645-6653.
41. Liu, W.; Zhao, X.; Cai, Z.; Han, B.; Zhao, D., Aggregation and stabilization of multiwalled carbon nanotubes in aqueous suspensions: influences of carboxymethyl cellulose, starch and humic acid. *RSC Advances* **2016,** *6* (71), 67260-67270.
42. Bouchard, D.; Zhang, W.; Powell, T.; Rattanaudompol, U.-s., Aggregation Kinetics and Transport of Single-Walled Carbon Nanotubes at Low Surfactant Concentrations. *Environ. Sci. Technol.* **2012,** *46* (8), 4458-4465.
43. Huang, P.; Jia, H.; Wang, T.; Xu, Y.; Zhang, L.; Wei, X.; Jia, H.; Wen, S.; Lv, K.; Liu, D., Effects of Modification Degrees on the Colloidal Stability of Amphiphilic Janus Graphene Oxide in Aqueous Solution with and without Electrolytes. *Langmuir* **2021,** *37* (33), 10061-10070.
44. Smith, B.; Wepasnick, K.; Schrote, K. E.; Cho, H.-H.; Ball, W. P.; Fairbrother, D. H., Influence of Surface Oxides on the Colloidal Stability of Multi-Walled Carbon Nanotubes: A Structure−Property Relationship. *Langmuir* **2009,** *25* (17), 9767-9776.
45. Konkena, B.; Vasudevan, S., Understanding Aqueous Dispersibility of Graphene Oxide and Reduced Graphene Oxide through pKa Measurements. *J. Phys. Chem. Lett.* **2012,** *3* (7), 867-872.
46. Tang, H.; Zhang, S.; Huang, T.; Zhang, J.; Xing, B., Mechanisms of the Aggregation of Graphene Oxide at High pH: Roles of Oxidation Debris and Metal Adsorption. *Environ. Sci. Technol.* **2021,** *55* (21), 14639-14648.
47. Zhang, J.; Xiong, C.; Li, Y.; Tang, H.; Meng, X.; Zhu, W., The critical contribution of oxidation debris on the acidic properties of graphene oxide in an aqueous solution. *J. Hazard. Mater.* **2021,** *402*, 123552.
48. Zhao, G.; Li, J.; Ren, X.; Chen, C.; Wang, X., Few-Layered Graphene Oxide Nanosheets As Superior Sorbents for Heavy Metal Ion Pollution Management. *Environ. Sci. Technol.* **2011,** *45* (24), 10454-10462.
49. Tombácz, E.; Tóth, I. Y.; Kovács, K.; Illés, E.; Szekeres, M.; Barna, B.; Csicsor, A.; Szabó, T., Striking analogies and dissimilarities between graphene oxides and humic acids: pH-dependent charging and colloidal stability. *J. Mol. Liq.* **2020,** *306*, 112948.
50. Gao, Y.; Yip, H.-L.; Chen, K.-S.; O'Malley, K. M.; Acton, O.; Sun, Y.; Ting, G.; Chen, H.; Jen, A. K.-Y., Surface Doping of Conjugated Polymers by Graphene Oxide and Its Application for Organic Electronic Devices. *Adv. Mater.* **2011,** *23* (16), 1903-1908.
51. Zhao, Q.; Zhu, X.; Chen, B., Stable graphene oxide/poly(ethyleneimine) 3D aerogel with tunable surface charge for high performance selective removal of ionic dyes from water. *Chem. Eng. J.* **2018,** *334*, 1119-1127.
52. Sun, Y.; Wang, Q.; Chen, C.; Tan, X.; Wang, X., Interaction between Eu(III) and Graphene Oxide Nanosheets Investigated by Batch and Extended X-ray Absorption Fine Structure Spectroscopy and by Modeling Techniques. *Environ. Sci. Technol.* **2012,** *46* (11), 6020-6027.
53. Dimiev, A. M.; Alemany, L. B.; Tour, J. M., Graphene Oxide. Origin of Acidity, Its Instability in Water, and a New Dynamic Structural Model. *ACS Nano* **2013,** *7* (1), 576-588.

54. Gaidukevic, J.; Aukstakojyte, R.; Navickas, T.; Pauliukaite, R.; Barkauskas, J., A novel approach to prepare highly oxidized graphene oxide: structural and electrochemical investigations. *Appl. Surf. Sci.* **2021,** *567*, 150883.
55. Araújo, M. P.; Soares, O. S. G. P.; Fernandes, A. J. S.; Pereira, M. F. R.; Freire, C., Tuning the surface chemistry of graphene flakes: new strategies for selective oxidation. *RSC Advances* **2017,** *7* (23), 14290-14301.
56. Zhao, J.; Liu, F.; Wang, Z.; Cao, X.; Xing, B., Heteroaggregation of Graphene Oxide with Minerals in Aqueous Phase. *Environ. Sci. Technol.* **2015,** *49* (5), 2849-2857.
57. Zeng, Z.; Wang, Y.; Zhou, Q.; Yang, K.; Lin, D., New insight into the aggregation of graphene oxide in synthetic surface water: Carbonate nanoparticle formation on graphene oxide. *Environ. Pollut.* **2019,** *250*, 366-374.
58. Yang, X.; Wang, Q.; Qu, X.; Jiang, W., Bound and unbound humic acids perform different roles in the aggregation and deposition of multi-walled carbon nanotubes. *Sci. Total Environ.* **2017,** *586*, 738-745.
59. Wu, Z.; Wang, Z.; Yu, F.; Thakkar, M.; Mitra, S., Variation in chemical, colloidal and electrochemical properties of carbon nanotubes with the degree of carboxylation. *J. Nanopart. Res.* **2017,** *19* (1), 16.
60. Wu, Z.; Mitra, S., Length reduction of multi-walled carbon nanotubes via high energy ultrasonication and its effect on their dispersibility. *J. Nanopart. Res.* **2014,** *16* (8), 2563.
61. Wang, M.; Gao, B.; Tang, D.; Sun, H.; Yin, X.; Yu, C., Effects of temperature on aggregation kinetics of graphene oxide in aqueous solutions. *Colloids Surf. A Physicochem. Eng. Asp.* **2018,** *538*, 63-72.
62. Tang, H.; Zhao, Y.; Yang, X.; Liu, D.; Shao, P.; Zhu, Z.; Shan, S.; Cui, F.; Xing, B., New Insight into the Aggregation of Graphene Oxide Using Molecular Dynamics Simulations and Extended Derjaguin–Landau–Verwey–Overbeek Theory. *Environ. Sci. Technol.* **2017,** *51* (17), 9674-9682.
63. Sun, B.; Zhang, Y.; Li, R.; Wang, K.; Xiao, B.; Yang, Y.; Wang, J.; Zhu, L., New insights into the colloidal stability of graphene oxide in aquatic environment: Interplays of photoaging and proteins. *Water Res.* **2021,** *200*, 117213.
64. Sun, B.; Zhang, Y.; Chen, W.; Wang, K.; Zhu, L., Concentration Dependent Effects of Bovine Serum Albumin on Graphene Oxide Colloidal Stability in Aquatic Environment. *Environ. Sci. Technol.* **2018,** *52* (13), 7212-7219.
65. Su, Y.; Yang, G.; Lu, K.; Petersen, E. J.; Mao, L., Colloidal properties and stability of aqueous suspensions of few-layer graphene: Importance of graphene concentration. *Environ. Pollut.* **2017,** *220*, 469-477.
66. Story, S. D.; Boggs, S.; Guiney, L. M.; Ramesh, M.; Hersam, M. C.; Brinker, C. J.; Walker, S. L., Aggregation morphology of planar engineered nanomaterials. *J. Colloid Interface Sci.* **2020,** *561*, 849-853.
67. Sotirelis, N. P.; Chrysikopoulos, C. V., Heteroaggregation of graphene oxide nanoparticles and kaolinite colloids. *Sci. Total Environ.* **2017,** *579*, 736-744.
68. Song, J.; Zeng, Y.; Liu, Y.; Jiang, W., Retention of graphene oxide and reduced graphene oxide in porous media: Diffusion-attachment, interception-attachment and straining. *J. Hazard. Mater.* **2022,** *431*, 128635.
69. Smith, B.; Wepasnick, K.; Schrote, K. E.; Bertele, A. R.; Ball, W. P.; O'Melia, C.; Fairbrother, D. H., Colloidal Properties of Aqueous Suspensions of Acid-Treated, Multi-Walled Carbon Nanotubes. *Environ. Sci. Technol.* **2009,** *43* (3), 819-825.
70. Shen, M.; Hai, X.; Shang, Y.; Zheng, C.; Li, P.; Li, Y.; Jin, W.; Li, D.; Li, Y.; Zhao, J.; Lei, H.; Xiao, H.; Li, Y.; Yan, G.; Cao, Z.; Bu, Q., Insights into aggregation and transport of graphene oxide in aqueous and saturated porous media: Complex effects of

cations with different molecular weight fractionated natural organic matter. *Sci. Total Environ.* **2019,** *656*, 843-851.
71. Saleh, N. B.; Pfefferle, L. D.; Elimelech, M., Influence of Biomacromolecules and Humic Acid on the Aggregation Kinetics of Single-Walled Carbon Nanotubes. *Environ. Sci. Technol.* **2010,** *44* (7), 2412-2418.
72. Park, C. M.; Wang, D.; Heo, J.; Her, N.; Su, C., Aggregation of reduced graphene oxide and its nanohybrids with magnetite and elemental silver under environmentally relevant conditions. *J. Nanopart. Res.* **2018,** *20* (4), 93.
73. Ntim, S. A.; Sae-Khow, O.; Witzmann, F. A.; Mitra, S., Effects of polymer wrapping and covalent functionalization on the stability of MWCNT in aqueous dispersions. *J. Colloid Interface Sci.* **2011,** *355* (2), 383-388.
74. Ntim, S. A.; Sae-Khow, O.; Desai, C.; Witzmann, F. A.; Mitra, S., Size dependent aqueous dispersibility of carboxylated multiwall carbon nanotubes. *J. Environ. Monit.* **2012,** *14* (10), 2772-2779.
75. Liu, X.; Xu, X.; Sun, J.; Duan, S.; Sun, Y.; Hayat, T.; Li, J., Interaction between Al2O3 and different sizes of GO in aqueous environment. *Environ. Pollut.* **2018,** *243*, 1802-1809.
76. Li, W.; Yu, J.; Zhang, S.; Tang, H.; Huang, T., The fate of aggregated graphene oxide upon the increasing of pH: An experimental and molecular dynamic study. *Sci. Total Environ.* **2022,** *851*, 157954.
77. Li, M.; Huang, C. P., Stability of oxidized single-walled carbon nanotubes in the presence of simple electrolytes and humic acid. *Carbon* **2010,** *48* (15), 4527-4534.
78. Khan, I. A.; Afrooz, A. R. M. N.; Flora, J. R. V.; Schierz, P. A.; Ferguson, P. L.; Sabo-Attwood, T.; Saleh, N. B., Chirality Affects Aggregation Kinetics of Single-Walled Carbon Nanotubes. *Environ. Sci. Technol.* **2013,** *47* (4), 1844-1852.
79. Jiang, Y.; Raliya, R.; Liao, P.; Biswas, P.; Fortner, J. D., Graphene oxides in water: assessing stability as a function of material and natural organic matter properties. *Environ. Sci.: Nano* **2017,** *4* (7), 1484-1493.
80. Huang, G.; Guo, H.; Zhao, J.; Liu, Y.; Xing, B., Effect of co-existing kaolinite and goethite on the aggregation of graphene oxide in the aquatic environment. *Water Res.* **2016,** *102*, 313-320.
81. Gao, Y.; Zeng, X.; Zhang, W.; Zhou, L.; Xue, W.; Tang, M.; Sun, S., The aggregation behaviour and mechanism of commercial graphene oxide in surface aquatic environments. *Sci. Total Environ.* **2022,** *806*, 150942.
82. Feng, Y.; Liu, X.; Huynh, K. A.; McCaffery, J. M.; Mao, L.; Gao, S.; Chen, K. L., Heteroaggregation of Graphene Oxide with Nanometer- and Micrometer-Sized Hematite Colloids: Influence on Nanohybrid Aggregation and Microparticle Sedimentation. *Environ. Sci. Technol.* **2017,** *51* (12), 6821-6828.
83. Du, T.; Adeleye, A. S.; Zhang, T.; Jiang, C.; Zhang, M.; Wang, H.; Li, Y.; Keller, A. A.; Chen, W., Influence of light wavelength on the photoactivity, physicochemical transformation, and fate of graphene oxide in aqueous media. *Environ. Sci.: Nano* **2018,** *5* (11), 2590-2603.
84. Chowdhury, I.; Mansukhani, N. D.; Guiney, L. M.; Hersam, M. C.; Bouchard, D., Aggregation and Stability of Reduced Graphene Oxide: Complex Roles of Divalent Cations, pH, and Natural Organic Matter. *Environ. Sci. Technol.* **2015,** *49* (18), 10886-10893.
85. An, S.; Zeng, Q.; Li, W.; Fortner, J., A graphene oxide Cookbook: Exploring chemical and colloidal properties as a function of synthesis parameters. *J. Colloid Interface Sci.* **2021,** *588*, 725-736.

86. Stankus, D. P.; Lohse, S. E.; Hutchison, J. E.; Nason, J. A., Interactions between natural organic matter and gold nanoparticles stabilized with different organic capping agents. *Environ. Sci. Technol.* **2011,** *45* (8), 3238-3244.
87. Hunter, R. J., *Foundations of Colloid Science*. 2nd ed.; Oxford University Press: 2001.
88. Luo, D.; Wang, F.; Alam, M. K.; Yu, F.; Mishra, I. K.; Bao, J.; Willson, R. C.; Ren, Z., Colloidal Stability of Graphene-Based Amphiphilic Janus Nanosheet Fluid. *Chem. Mater.* **2017,** *29* (8), 3454-3460.
89. Sato, Y.; Kusaka, Y.; Kobayashi, M., Charging and Aggregation Behavior of Cellulose Nanofibers in Aqueous Solution. *Langmuir* **2017,** *33* (44), 12660-12669.
90. Kobayashi, M.; Sato, Y.; Sugimoto, T., Effect of pH and electrolyte concentration on sol–gel state of semi-dilute aqueous cellulose nanofiber suspension: an interpretation based on angle-dependent DLVO theory. *Colloid and Polymer Science* **2022,** *300* (8), 953-960.
91. Lu, N.; Mylon, S. E.; Kong, R.; Bhargava, R.; Zilles, J. L.; Nguyen, T. H., Interactions between dissolved natural organic matter and adsorbed DNA and their effect on natural transformation of Azotobacter vinelandii. *Sci. Total Environ.* **2012,** *426*, 430-435.
92. Labille, J.; Thomas, F.; Milas, M.; Vanhaverbeke, C., Flocculation of colloidal clay by bacterial polysaccharides: effect of macromolecule charge and structure. *J. Colloid Interface Sci.* **2005,** *284* (1), 149-156.
93. Zhang, Z.; Pfefferle, L.; Haller, G. L., Comparing characterization of functionalized multi-walled carbon nanotubes by potentiometric proton titration, NEXAFS, and XPS. *Chinese J. Catal.* **2014,** *35* (6), 856-863.
94. Rourke, J. P.; Pandey, P. A.; Moore, J. J.; Bates, M.; Kinloch, I. A.; Young, R. J.; Wilson, N. R., The Real Graphene Oxide Revealed: Stripping the Oxidative Debris from the Graphene-like Sheets. *Angew. Chem. Int. Ed.* **2011,** *50* (14), 3173-3177.
95. Fogden, S.; Verdejo, R.; Cottam, B.; Shaffer, M., Purification of single walled carbon nanotubes: The problem with oxidation debris. *Chem. Phys. Lett.* **2008,** *460* (1), 162-167.
96. Verdejo, R.; Lamoriniere, S.; Cottam, B.; Bismarck, A.; Shaffer, M., Removal of oxidation debris from multi-walled carbon nanotubes. *Chem. Commun.* **2007,** (5), 513-515.
97. Delgado, A. V.; González-Caballero, F.; Hunter, R. J.; Koopal, L. K.; Lyklema, J., Measurement and Interpretation of Electrokinetic Phenomena (IUPAC Technical Report). *Pure Appl. Chem.* **2005,** *77* (10), 1753-1805.
98. Gao, H.; Zhong, S.; Dangayach, R.; Chen, Y., Understanding and Designing a High-Performance Ultrafiltration Membrane Using Machine Learning. *Environ. Sci. Technol.* **2023**.
99. Wang, R.; Zhang, S.; Chen, H.; He, Z.; Cao, G.; Wang, K.; Li, F.; Ren, N.; Xing, D.; Ho, S.-H., Enhancing Biochar-Based Nonradical Persulfate Activation Using Data-Driven Techniques. *Environ. Sci. Technol.* **2023,** *57* (9), 4050-4059.
100. Yang, R. X.; McCandler, C. A.; Andriuc, O.; Siron, M.; Woods-Robinson, R.; Horton, M. K.; Persson, K. A., Big Data in a Nano World: A Review on Computational, Data-Driven Design of Nanomaterials Structures, Properties, and Synthesis. *ACS Nano* **2022,** *16* (12), 19873-19891.

852 Table of Contents Graphic

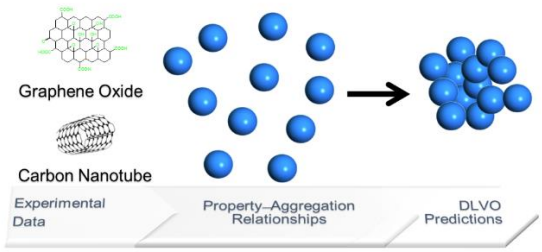

853